Chapter

Floating Cities Bridge in 2050

Faham Tahmasebinia, Yutaka Tsumura, Baichuan Wang, Yang Wen, Cheng Bao, Samad Sepasgozar and Fernando Alonso-Marroquin

Abstract

A floating cities bridge is designed to connect two floating cities or nearby land to resolve the problem of shortage of construction land due to an increase of population and sea level. The Yumemai floating bridge is referenced as a sample structure; the member sizes and dimensions are modified to suit the need of the project. A finite element structure is built using Strand7, which includes dead load, live load, tidal wave, and wind load. Based on the loads, both static and dynamic analyses are conducted to determine the stress and deflection of the structure. The report outlines the modeling techniques, element types, and analysis solvers used in modeling and analyzing the structure. This report discusses the results obtained from the analysis. The advanced material with low density applied is introduced, which has a good resistance of corrosion and high strength. The main objective of the current chapter is to suggest and design the procedure which can be used as floating structural elements in the future.

Keywords: floating cities bridge, finite element structure

1. Introduction

According to the UN DESA report [1, 2], it is estimated that the world population will reach 9.7 billion in 2050 and 11.2 billion in 2100. This exploding growth of the population brings a great pressure on the demands of construction land. In addition, an increasing sea level aggravates the pressure on the shortage of the land. Sea level will rise as much as 50 cm by 2050 as the report of midrange projections indicated. Floating cities are required to release the intensity of using lands and under such circumstance, and bridges will be an essential infrastructure connecting floating cities. Since floating cities are a mobile structure, the bridge also needs to be mobile and flexible in terms of placement; the solution proposed in the report is a floating bridge which can move around with floating cities and be rapidly deployed when needed. The bridge is designed as modular bridge; thus multiple bridge module can be connected to achieve the desired length depending on the distances required. A floating bridge has a number of advantages over the conventional bridge, for example, marine environment remaining undisturbed; easier construction, as most of construction process can be done onshore; and floating structures being immune to earthquake.

A successful floating bridge, Yumemai Bridge in Japan [1], is referenced as a basic model. Dimensions and sizes are modified to suit the need of the project. The behavior of isolated bridge module is investigated as an initial step to model the bridge. The report presents the Strand7 model, the introduction of the new material, and analysis results associated with the static and dynamic behaviors of the bridge.

2. Structural system

In **Figure 1**, the length of one bridge module is 382 m, width is 38.8 m, and height is 65.5 m, respectively. The number of lanes is designed as four. The pontoon size is 7.5 × 58 × 58 m. The bridge is comprised of a bridge deck which is supported via six columns at each end. The bridge deck between pontoons is hanged by vertical members at 23.3 m intervals. The vertical members are necessitated for this larger-span floating bridge to decrease deflection in the center of the bridge. To control the deflection, the deck itself has a parabolic shape which has a 640 mm rise in the center. The vertical members are supported by the larger-span arch structures. The loads applied to the bridge deck in service are transferred into the vertical member and then passed into the arch structure which carries the load in compression. Finally, the load is carried by the pontoon via the load paths of columns.

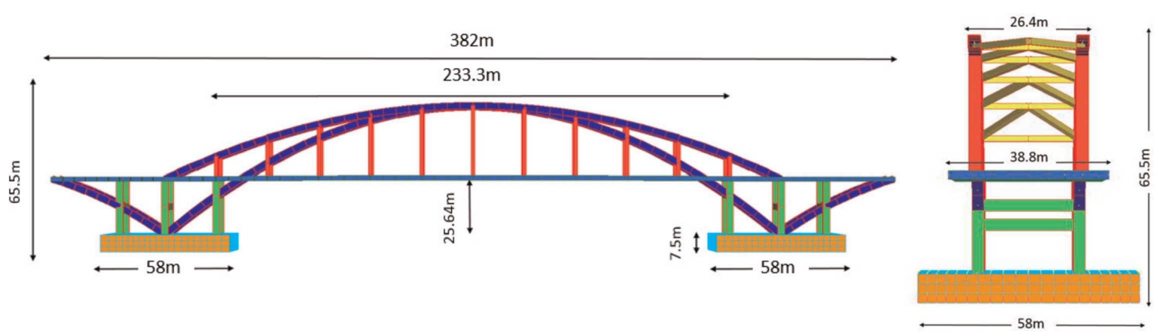

Figure 1.
Dimensions of the bridge.

3. Materials

In a floating offshore structure, the self-weight and corrosion resistance are the two most critical parameters that decide the material to be used in the structure. New novel materials are adopted in this floating bridge, which has characteristics of light, high corrosion resistance, and high strength. These materials enable to reduce the self-weight and increase the durability in aggressive ocean environment. The two main materials used in the floating bridge are nanocrystalline steel and carbon fiber-reinforced plastic (CFRP).

Nanocrystalline steel is chosen as it has an extremely high yield strength. It contains a significant volume fraction of interfacial regions separated by nearly perfect crystals [3]. Since the atomic structure of the grain boundary differs greatly from the inside of the grain, such steel full of grain boundary shows properties that are quite different from those full of conventional metals [4]. The deformation of the metal material is carried out by a sliding motion of lattice defect called as dislocation. In the bulk nanocrystalline metal, the individual crystals are strongly bound by the grain boundaries, and the energy of the dislocation also changes; its behavior surpasses any metals available today. Bulk nanocrystalline steel shows

Material used	Yield strength (MPa)	Yong modulus (GPa)	Density (kg/m^3)
Bulk nanocrystalline steel	2000	200	7850
Concrete (40 MPa)	40	34.5	2400
CFRP	1300	300	16.5

Table 1.
Material properties.

strength which is four times higher than that of conventional metal which is currently developed [4]. It is used for all metal structures of the bridge [3] and is assumed to have a yield strength of 2 GPa which is four times greater than the current structural steel. Such high-strength material allows to reduce the self-weight drastically, by enabling to reduce the cross-sectional area of the member. And also nanocrystalline steel has an excellent corrosion resistance which makes it the ideal material for an offshore floating structure.

Another material used is carbon fiber-reinforced polymer composites (CFRP). It is an extremely strong and light fiber-reinforced plastic which contains carbon fibers. The yield strength of the CFRP in tension and compression are 1600 and 1300 MPa, respectively, Young's modulus 300 GPa, and Poisson' ratio 0.3 with a density of 1.65 g/cm^3 [5]. This material is utilized in the pontoon. Convectional 40 MPa concrete is also used in the columns. The properties of the materials used are summarized in **Table 1**.

4. Loads

4.1 Load analysis

When designing a floating bridge, it is necessary to consider the effects of dead load, live load, wind load, and tidal wave load on the behavior of the bridge. The vertical load resulted from self-weight, and live load is counteracted via buoyancy force. The buoyancy force is generated by using the large pontoons. The live load is caused by traffic, and the truss bridge deck carries the traffic load directly. Wind loads are perpendicular to the face of the members; on the other hand, wave load is applied to the face and side surface of the pontoon, and both wind and tidal wave loads are time-dependent load and hence vary with time.

The bridge deck is supported by the six columns and the vertical cables. And the cable is hanged from two main arch structures. Six columns are supported via large pontoons. The pontoons also support the two main arch structures.

4.2 Calculation of loads

4.2.1 Dead load

Dead load is the self-weight of the floating bridge, since all the used materials' sizes, densities, and other properties are inputted in Strand7; the dead load is calculated automatically by Strand7 under the effect of gravity g = 9.81 m/s^2.

4.2.2 Live load

The floating bridge is catered to connect two floating cities with four lanes for carrying traffic. The estimated traffic loading is determined in according to the AS

5100.2 clause 7.2.4 [6]. The load model M1600 was chosen to determine the traffic load, which is considered as the worst case. This load model means that the bridge is fully loaded with trucks. The uniformly distributed component of the M1600 moving traffic load shall be continuous under the axle group loads and shall be considered as uniformly distributed over the width of a 3.2 m standard design lane.

To make the calculation simple, the total load was applied on the bridge deck as a pressure load. According to the standard, the initial step is to calculate the traffic load for a portion of the bridge and then determine the total load being applied in the whole structure. The load, given for the load model of M1600 from the code, includes the axle group loads of 360 kN and uniformly distributed load of 6 kN/m. There are four lanes of traffic this load multiplied with 4. The total length of the bridge is 382 m, and the bridge is subdivided into 16.4 segments. For each segment, the load with 6360 kN is applied according to the standard. Finally, the total load is 10 kPa in that the load for each segment is multiplied by 15.3.

Length of each segment

$$L = 1.25 \times 8 + 3.75 + 6.25 + 5 = 25\text{m} \tag{1}$$

Number of segment in the signed bridge

$$382 \div 25 = 15.3 \tag{2}$$

Total load on the bridge

$$(360\ \text{kN} \times 4 + 6\ \text{kN} \times 25) \times 15.3 \times 4 = 97308\ \text{kN} \tag{3}$$

Equivalent pressure

$$97308 \div 25 \div 382 = 10\ \text{kPa} \tag{4}$$

4.2.3 Wind load

The design wind load speed is determined based on the AS1170 [7], which is 57.8 m/s ARI of 1000-year designed wind speed. The wind load is applied on every member as a pressure load including the deck face that is perpendicular to the wind direction.

Designed wind speed

$$V_{des,\theta} = V_R \times M_d \times (M_{z,cat} \times M_s \times M_t) = 46 \times 1.2564 \times 1 \times 1 \times 1 = 57.8\ \text{m/s} \tag{5}$$

Pressure on the side of the deck

$$P = (0.5\rho_{air})[V_{des,\theta}]^2 C_{fig} C_{dyn} \tag{6}$$

$$C_{fig} = C_{dyn} = 1 \tag{7}$$

Side

$$P = \left(0.5 \times \frac{1.2kg}{m^3}\right)\left(\frac{57.8m}{s}\right)^2 = 2.005\ \text{kPa} \tag{8}$$

4.2.3.1 Bridge deck uplift and downlift

The wind load applied in the bridge deck is simplified, and the external coefficients ($C_{p,e}$) are −1.3 (up) for top bridge deck and −1.2 (down) for bottom bridge deck which is not varied with position assumedly.

$$C_{fig} = C_{dyn} = -1.3 \tag{9}$$

$$P_{uplift} = \left(0.5 \times 1.2\ \mathrm{kg/m^3}\right)(57.8)^2 \times (-1.3) = -2.606\ \mathrm{kPa} \tag{10}$$

$$P_{downlift} = \left(0.5 \times 1.2\ \mathrm{kg/m^3}\right)(57.8)^2 \times (-1.2) = -2.405\mathrm{kPa} \tag{11}$$

4.2.4 Tidal wave load

The ocean water flows through the pontoon and causes two types of load that are the frontal drag force and the side drag force.

In order to consider worst case, assuming full pontoon is subjected to tidal wave load and this scenario cause the maximum adverse load. According to the AS5100 [6], the load is calculated as below. The velocity of water is assumed typical wave speed under severe storm condition, 14.8 m/s [7] .

Design drag force (in front of pontoon)

$$F_d = 0.5C_d V^2 A_d \tag{12}$$

where $C_d = drag\ efficient$ and $A_d = wetted\ area\ of\ the\ pontoons\ normal\ to\ the\ water\ flow$.

$$C_d = 1.4\ (square\ shape) \tag{13}$$

$$A_d = 7.5\mathrm{m} \times 58\mathrm{m} = 435\mathrm{m}^2 \tag{14}$$

$$P = 0.5C_d V^2 = 0.5 \times 1.4 \times (14.83\mathrm{m/s})^2 = 154\mathrm{Pa} \tag{15}$$

$$F_D = 0.5C_d V^2 A_s = 154 \times 435\mathrm{m}^2 = 66968\mathrm{N} \tag{16}$$

4.2.5 Side drag on pontoon

$$\mathrm{F_L} = 0.5\mathrm{C_s}\mathrm{V}^2\mathrm{A_L} \tag{17}$$

where $C_s = drag\ efficient$ and $A_L = wetted\ area\ of\ the\ pontoons\ normal\ to\ the\ water\ flow$.

$$C_s = 0.9, for\ \theta_w \leq 30° \tag{18}$$

$$A_L = 58\mathrm{m} \times 7.5\mathrm{m} = 435\mathrm{m}^2 \tag{19}$$

$$P = 0.5 \times (0.9) \times (14.83\mathrm{m/s})^2 = 100\mathrm{Pa} \tag{20}$$

$$F_L = 0.5C_s V^2 A_L = 100 \times 435\mathrm{m}^2 = 43051\mathrm{N} \tag{21}$$

4.2.6 Maximum buoyancy

This floating bridge, compared with normal sea bridge, is dependent on the buoyancy force to support the structure instead of installing pile foundation at the seabed. A pontoon built below the column of the bridge is submerged in the ocean, and it generates a buoyancy force that can balance the opposite vertical load. These vertical loads result from self-weight, wind load, live load, and traffic load. The size of the pontoon is 58 × 58 × 7.5 m; the specific weight of the seawater may be taken to be 10.05 kN/m^3. The maximum buoyancy of the pontoon is calculated as follows:

$$V = 7.5\text{m} \times 58\text{m} \times 58\text{m} = 10765\text{m}^3 \tag{22}$$

$$F_{buoyancy} = \rho g V = 10.9\text{kN/m}^3 \times 10765\text{m}^2 = 108188\text{kN} \tag{23}$$

5. Modeling element and material

5.1 Mesh and mesh quality

The bridge deck is made by plate elements, and all the others are made by using beam elements. All the elements are subdivided to the shape as square as possible; the deck and columns as well as the columns and pontoon have to align with each other to ensure they are entirely connected to each other to get an accurate result and avoid any mesh discontinuity.

5.2 Nodal constraints

The boundary conditions for the left end which are connecting Sydney land, the DX, DZ, RX, and RY are fixed. The other side which is connecting the floating city or next bridge module is free in both translation and rotation. To carry out linear static, natural frequency, and harmonic response analysis, the base of the pontoon is assumed to be fixed in DY, otherwise static condition cannot be established. In nonlinear transient dynamic analysis, the constraints at the base of the pontoon are removed, and pontoon is free in all directions; the constraints are replaced with buoyancy pressure to simulate the dynamic behavior of the bridge on the water.

5.3 Element types

5.3.1 Bridge deck

To comply with AS5100 deflection control and minimize deflection, the deck itself has a parabolic shape with a 640 mm rise in the center. This allows to reduce the deflection under both serviceability and ultimate states. To simplify the model, the truss deck is modeled as a plate element; the truss is assumed to have a relative density of 0.025, and the effective elastic modulus is obtained by the following formula [8]:

$$E_L = \frac{1}{9}\rho_L E_0 \tag{24}$$

where ρ_L is the relative density and E_0 is the elastic modulus of parent material. The pontoon relative density is set as 0.05 and the same procedure is applied.

5.3.2 Main arch

The dimension of the main arch is decided first by solving the simple arch structure applying only live load calculated above; once the maximum force is obtained by simple statics, the required cross-sectional area to carry the applied load is calculated. Outer dimension of the member is based on the referenced structure Yumemai Bridge, and the thickness of the member is calculated by distributing the area required around four sides of the square hollow section member. Then the member thickness is modified to control deflection, and, finally, the main arch was modeled using a beam element with the dimension of 3 × 3 × 0.03 m RHS.

5.3.3 Vertical members

There are 11 vertical members connecting the main arch and the bridge deck on both sides; the height of the members is changing along the bridge with the different positions under the arch; the cross section is 1.5 × 0.75 × 0.015 m. Beam element is used.

5.3.4 Cross member

Between the two main arches, the cross member was applied by using the beam element with the dimension of 0.75 × 0.75 × 0.01 m RHS.

5.3.5 Column

The deck and pontoon were connected by six columns on each end of the bridge; the columns are a 3 × 3 m solid concrete which was modeled using a beam element.

5.3.6 Pontoon

The size of the pontoon is 58 × 58 × 7.5 m cuboid modeled by a solid element in Strand7. Initial submerged depth is set as 4.5 m, i.e., 3 m from the top of the pontoon; the bridge will then adjust itself to gain equilibrium with water pressure, and the final submerged depth will be 4 m.

Dimension and material properties of each element are summarized in **Table 2**.

Modeled element	**Modeling shape**	**FEM element**	**Material used**	**Yong modulus (GPa)**	**Density (kg/m^3)**	**Geometric properties (m)**
Main arch	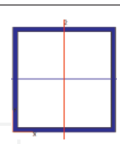	Beam	Bulk nanocrystalline steel	200	7850	3 × 3 × 0.03
Vertical member	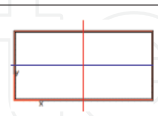	Beam	Bulk nanocrystalline steel	200	7850	1.5 × 0.75 × 0.015
Cross member	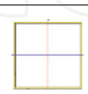	Beam	Bulk nanocrystalline steel	200	7850	0.75 × 0.75 × 0.01
Column	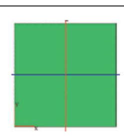	Beam	Concrete (40 MPa)	34.5	2400	3 × 3
Deck	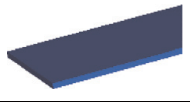	Plate	Bulk nanocrystalline steel (Truss)	0.556	196.25	2 m thickness
Pontoon	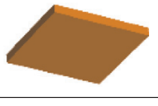	Solid	CFRP	1.67	82.5	58 × 58 × 7.5

Table 2.
Element properties.

6. Numerical analysis

6.1 Linear static analysis

The linear static solver is used to analyze the effects of different combination load cases. According to AS1170, the combination load cases are calculated basing on the dead load, live load, and wind load; two critical load cases 1.0G dead load only (serviceability state) and 1.2G + 1.5Q (ultimate state) are considered to check the adequacy of the structure.

By comparing the results for different combination load cases, it is found that load case 2 (ultimate state) has significant effects on the structure. **Figure 2** shows that the maximum displacement under ultimate state is 1600 mm. Note that the bridge deck is raised by 640 mm, so under the ultimate condition, the deflection of the bridge deck is 960 mm that is below the flat level. It is also found that the maximum stress is 254 MPa compression which is located in the root of the main arch structure. In **Figure 3**, under serviceability state (1.0 G), the maximum deflection of the deck is 505 mm which is 95 mm above the flat level. AS5100 [6] limits the deflection under serviceability condition to be "deflection/span < 1/600"; the bridge complies the deflection limit. The maximum stress under serviceability condition is found to be 82.7 MPa.

The linear static analysis showed that the material dimensions are satisfactory, both in terms of strength and deflection, under serviceability and ultimate states.

6.2 Natural frequency analysis

The natural frequency is defined as free vibrations of an elastic body. If the frequency of the applied load is identical as the natural frequency of the structure, hence the amplitude of vibration increases manifold. It is significantly important to find the critical frequency that causes the maximum deflection. Two hundred different natural frequencies under 12 Hz are found of which 173 of them are

Figure 2.
Stress and deflection under ultimate state.

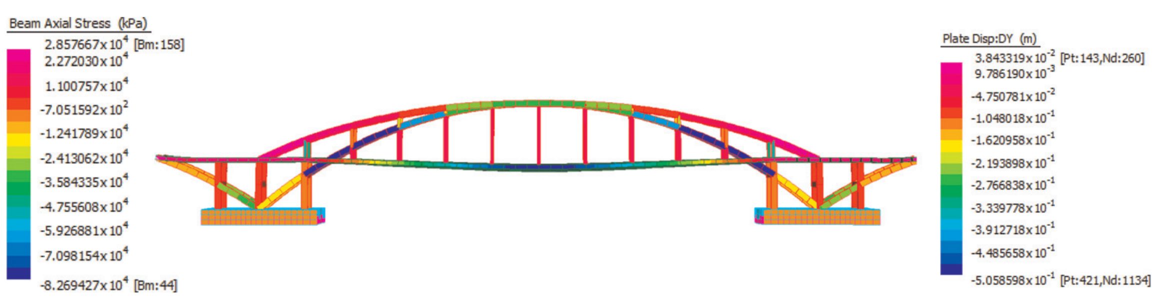

Figure 3.
Stress and deflection under serviceability state.

converged; the minimum mass participation factor is 85.08%. The typical ocean wave has a frequency ranging from 0.1 to 5 Hz [8]. The analysis covers this area of the frequencies. These frequencies found are used to conduct harmonic response analysis. The first 20 modes of natural frequencies are listed in **Table 3**.

6.3 Harmonic response analysis

In floating structure the effect from the earthquake is minimal as the water acts as a base isolation material; hence any ground movement will not be transferred to the structure, but what matters to the structure is the daily wave and wind load. As mentioned previously, the typical wave has a frequency between 0.1 and 5 Hz. Natural frequency analysis in **Figure 4a** showed that there are a number of natural frequencies within this range; when the wave frequency coincides with the natural frequency, the effect on the structure could be significant and cause devastating damage. Thus it must be investigated. Harmonic response solver is used to test the effect of sinusoidally varying the load under 7.5 Hz; the dominant varying load will be the wave load, however, to be conservative, and wind loads are also assumed to be a varying load.

The deflection at the center of the deck versus different frequencies is plotted in **Figure 4a**. The harmonic response analysis has shown the frequency of 0.51789 Hz produced the largest deflection, and it can be said that the structure is most sensitive to this frequency. **Figure 4b** shows deflection contour under such frequency; the maximum displacement due to the frequency is found to be 0.456 m since the deflection caused by the load is relatively small considering the large span of the bridge, and it also complies the 1/600 deflection limit. The bridge will still be able to serve its purpose.

6.4 Nonlinear transient dynamic analysis

The nonlinear transient dynamic solver is used to analyze the effects of the combination dynamic loads on the floating bridge. Under transient dynamic circumstance, the effects of the wind load, wave load, and buoyancy force have a significant impact on the bridge deflection and the maximum stress within the structure. Both wind load and wave load are varied with time and utilizing load

Mode	Natural frequency (Hz)	Mode	Natural frequency (Hz)
1	0.0461395	11	1.83116
2	0.349325	12	1.84217
3	0.517894	13	1.96018
4	0.778749	14	2.06939
5	0.929989	15	2.20666
6	1.01908	16	2.29274
7	1.16268	17	2.36013
8	1.21482	18	2.44297
9	1.46656	19	2.52935
10	1.51455	20	2.61975

Table 3.
Natural frequency of the bridge.

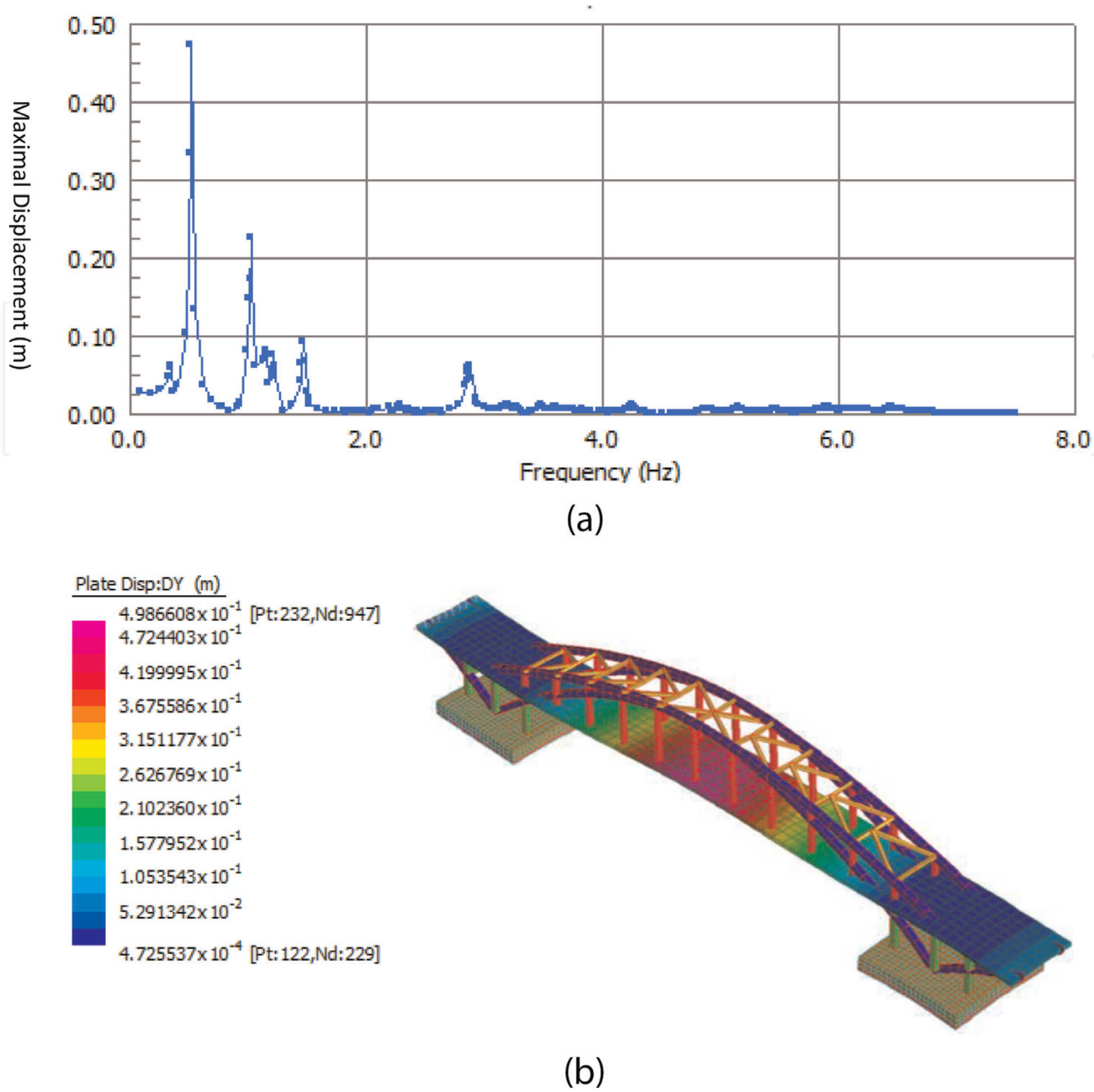

Figure 4
(a) Displacement versus frequency. (b) Displacement contour under varying load f = 0.51789 Hz.

factor variation. The buoyancy force is varied depending on the vertical position of the bridge.

The applied loads, wave load, wind load, and live load, vary with respect to time in nonlinear transient dynamic analysis, and their variation is shown in **Figure 5a–d**. Variation is expressed as a load factor from 0 to 1, one meaning maximum designed load. Tidal wave load is considered as a simple harmonic motion. The designed wave velocity is the typical velocity (14.83 m/s) under storm condition, period of 14.3 s (0.699 Hz), wavelength of 212.6 m, and amplitude of 7.4 m [5]. The wind speed variation is considered as a storm day wind profile in Sydney harbor on October 05, 2017 [8], and shrunk into 140 s as shown in **Figure 5c**; load factor is the ratio between designed wind speed and applied wind speed. One means applied wind speed = designed wind speed (i.e., 58 m/s). The traffic load also varies the simulating traffic condition on the bridge as shown in **Figure 5d**. The trapezoidal loading curve simulates the accumulation of traffic caused by red traffic light and clearing off when the light turns green.

Normal pressure is applied at the bottom of the pontoon to simulate the buoyancy. One kilopascal is applied and factored by its vertical position. Load factor is shown below.

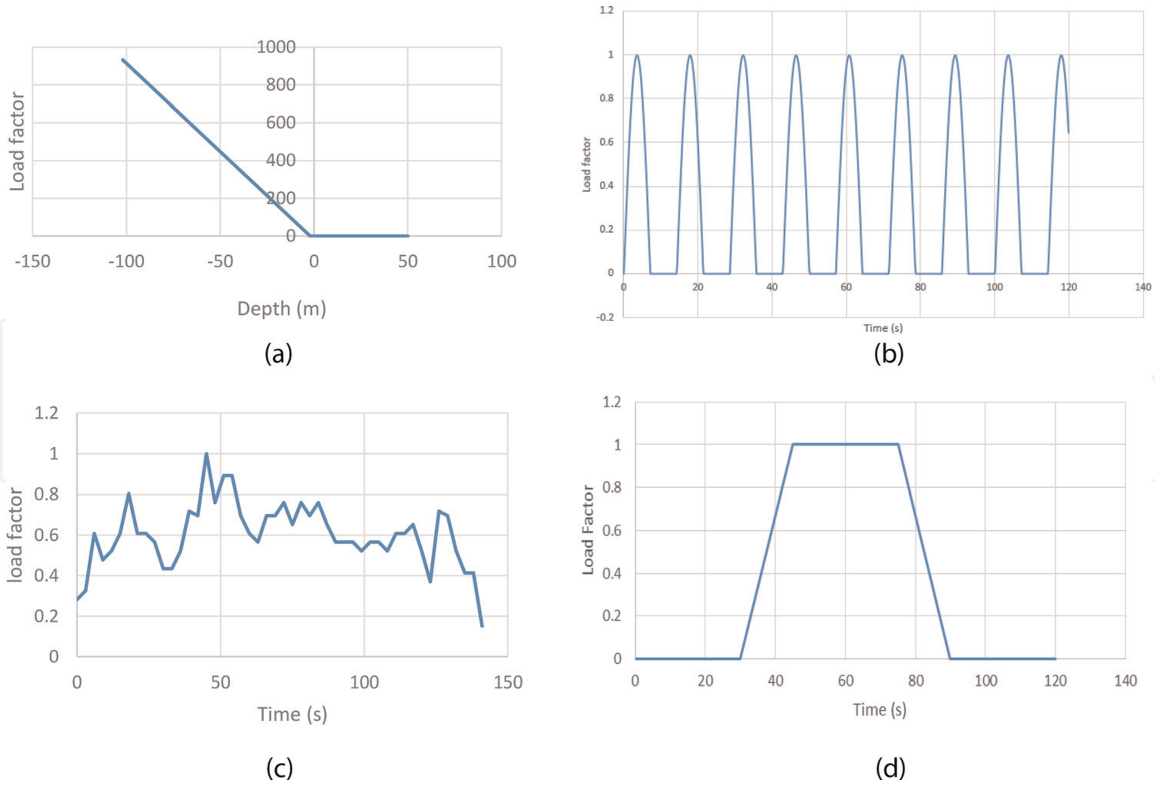

Figure 5
(a) Load factor versus position (buoyancy). (b) Load factor versus time (wave load). (c) Load factor versus time (Wind load)—storm day wind profile in Sydney harbor on 10/05/2017. (d) Load factor versus time (Traffic load)—simulates the accumulation of traffic and clearing off.

7. Results

The behavior of the bridge under dynamic condition is modeled for 2 minutes. The bridge must satisfy the following criteria for it to be successfully designed. Firstly, the maximum stress on the member does not exceed the member capacity. Secondly, the buoyancy provided by the pontoon is able to carry the maximum designed load. And finally, the deflection under serviceability condition complies AS5100 [6].

7.1 Pontoon displacement

As shown in **Figure 6**, the initial oscillation from 0 to 30 s is due to bridge adjusting itself to an equilibrium position; after 30 s the pontoon submerged due to increasing live load and stays at a constant around −2.2 m. At 75 s the pontoon starts float back up as live load is decreased, and about 90 s the bridge is at equilibrium with its self-weight; the small oscillation observed from 90 to 120 s is due to the applied wave load and wind load. As the water level is set at −3 m and the top of the pontoon is 0 m. The maximum displacement of the pontoon can be found at 45 s with a displacement of −2.4 m; at this point the top of the pontoon is 0.6 m above the water level. The bridge is in equilibrium when the pontoon is submerged 4.5 m in the water, and there is 3 m of extra buoyancy, for live, wind, and wave loads, which is equivalent to 200,000 kN of force. When fully designed live load is applied, there is still 0.6 m of extra buoyancy which is equivalent to 40,000 kN, and therefore the size of the pontoon is satisfactory providing sufficient buoyancy under all condition.

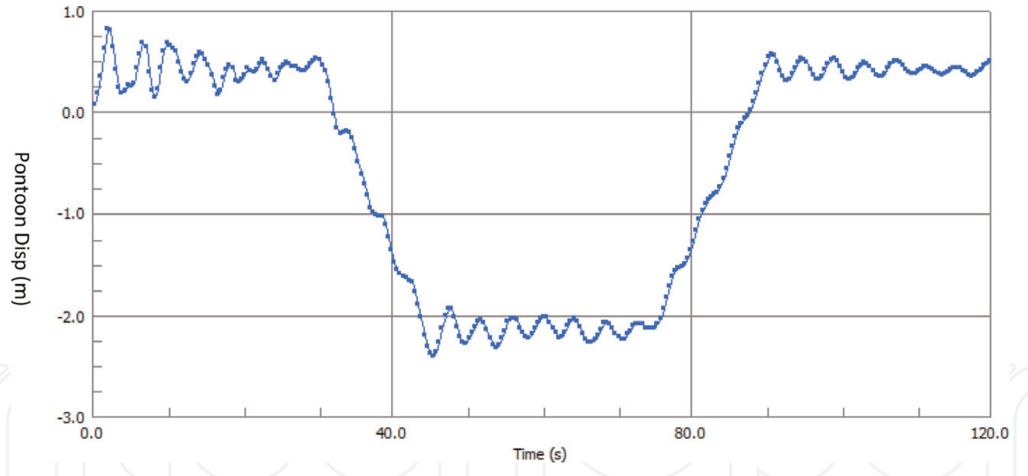

Figure 6.
Displacement at the top of pontoon.

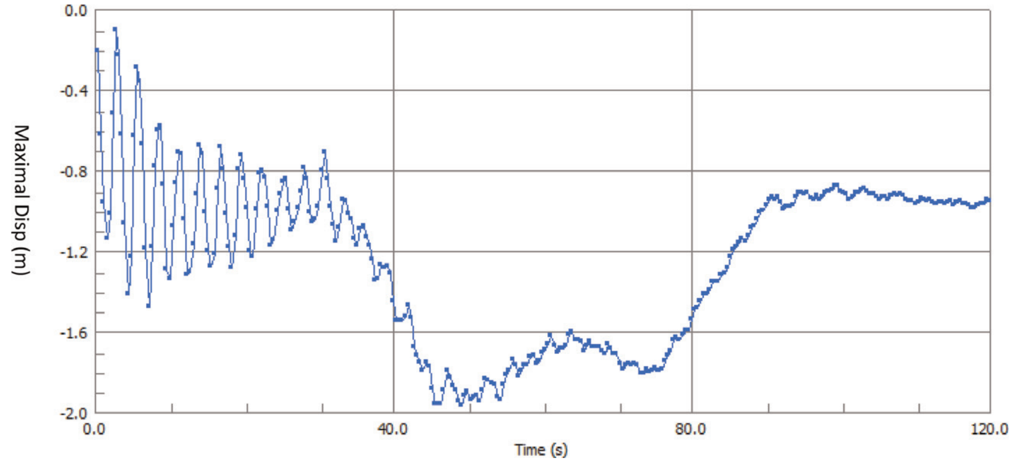

Figure 7.
Deflection at the mid-span of the deck versus time.

7.2 Deck deflection

By comparing the relative displacement of the pontoon and the deck, the deflection due to self-weight, wave load, and wind load can be isolated.

As shown in **Figure 7** (90–120 s), without traffic load, the deflection of the plate is around 900 mm. Given that the deck has risen by 640 mm in the mid-span, the deck is 260 mm lower than the flat level, and it complies with serviceability deflection of AS5100 [6]. Hence the deflection is also satisfactory. It can be seen that when designed traffic load is applied (45–75 s), the deflection of the plate will increase to 2 m meaning the deck is 1360 mm lower than the flat level. This is greater than the deflection limit of AS5100 [6]. However such case is regarded as an ultimate state; hence the 1/600 deflection limit does not apply.

7.3 Maximum stress

The maximum axial force is found at the root of the main arch structure. Axial force for the member is shown in **Figure 8**. It is observed that the axial force changes with time. The maximal tension (positive) is approximately 5000 kN, and the maximal compression force (negative) is 80,000 kN. The maximum stress can be calculated by dividing the cross-sectional area of the main arch, and hence the maximum stress is 225 MPa.

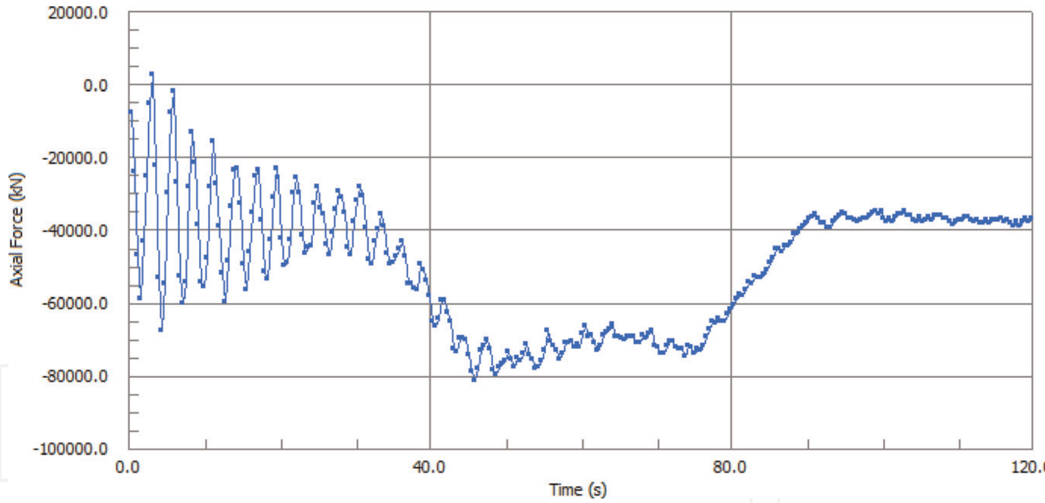

Figure 8.
Axial force versus time.

Loading condition	Maximum stress (MPa)	Maximum deflection (mm)
Linear static analysis (1.2G + 1.5Q)	254	960
Nonlinear transient dynamic (45–75 s)	225	1360
Linear static analysis (1.0G)	82.7	−100
Nonlinear transient dynamic (90–120 s)	112	260

Table 4.
Maximum stress and deflection under different loading condition.

The applied dynamic loads include the traffic load, wind load, and tidal wave load which are 10, 2.5, and 0.15 kPa, respectively. The dominant load is the live load. In the figures related to load factor, it is observed that both wind load and tidal wave load are consistently being applied to the structure. After 30 s, the live load is increasingly imposed to the structure. The figure of displacement and stress can show the effects of the load.

Initially the deflection and stress are caused by the movement of the bridge adjusting the position. Then, the live load starts to influence on the bridge after 30 s. Since the traffic load is significantly larger than other dynamic load, the effect on the displacement and stress is dominated by the traffic load. It is observed that the displacement and stress stay almost constant when the traffic load factor becomes 1 (i.e., when fully designed traffic load is applied) and kept constant from 45 to 75 s. After the traffic load is fully cleared at 90 s, the displacement and stress observed are solely due to wind load and tidal wave load. The stress and displacement fluctuate at the period of the wave load. However, the variation is fairly limited as the bridge contains a large mass and the effect from projected area pontoon is small. Comparison between worst-case static analysis and dynamic analysis is shown in **Table 4**.

8. Discussion

It is interesting to note that in worst-case scenario in linear static analysis which is ultimate load case of 1.2G + 1.5Q produced largest stress in the main arch with 254 MPa with 960 mm of deflection at the mid-span of the deck. On the other hand, in dynamic analysis, the maximum stress is found to be 225 MPa which is lower than the static analysis, and yet the deflection is found to be 1360 mm which is much greater than the linear static analysis. This larger deflection can be explained by the superposition effect that is the sum of response of each stimulus individually. When the peak of wind/wave load coincide with the each other, and since wave load is modeled as sine function with frequency of 0.699 Hz and as natural frequency solver has shown that the one of the natural frequency of the bridge is 0.69798 Hz and is very close to the frequency of the applied wave (0.699 Hz). As a result, the bridge will resonate with the wave loads and produce a larger deflection. This is also evident in the maximum stress in the member; the maximum on the member is fundamentally the function of the load applied; in ultimate state the total applied load 1.2G + 1.5Q produces a greater total load which results in a higher stress in the member. This means the large deflection is not caused by applied load but rather oscillation of the bridge, resonating the wave load.

The maximum stress presented in a member is 254 MPa; the conventional structural steel will be sufficient under such load. However in an aggressive marine environment, the corrosion of the member will be a large issue, and therefore nanocrystalline steel is still the preferred option. However knowing that the stress is in such magnitude, nanocrystalline aluminum will also be an ideal candidate as it is three times lighter than steel. And by the utilizing nanocrystallization, the low yield stress of conventional aluminum could be overcome, and also aluminums are inheritably a more resilient corrosion than steel. There is a drawback of using aluminum such as them having lower elastic modulus; since nanocrystallization does not influence the elastic modulus of the material, the deflection could be a significant issue. Hence size and dimension of the member need to be modified to compensate for the lower elastic modulus.

9. Conclusions

The floating bridges are a practical infrastructure connecting floating cities, which resolve the potential issue of the land shortage due to an increasing population and sea level. The pontoon is utilized to support the structure instead of pile foundation being fixed in the seabed which greatly contributes mobility and thereby feasibility of the floating cities. The primary concept of the designed bridge is “flexibility.” The modular design allows easy adjustment to meet specific local demands of a wider range of situation, which renders the structure a suitable solution to the floating cities bridge.

The investigation on effects of static loading and dynamic loading (wind, wave, and traffic loads) on the structure was performed. And it was found that dynamic load produced the largest deflection due to superposition effects and the static loads produced the largest stress. In either case, the design of the bridge fulfills the requirements of deflection, pontoon displacement, and maximum stress. This floating bridge can be referenced for future real project.

In addition, the software analysis cannot conduct the analysis of the influence of the turbulence caused by fluid flowing through the bridge, including wind and water. Computational fluid dynamic (CFD) modeling can be done, and/or a prototype of a floating bridge is necessarily built to simulate a real scenario of wind and ocean wave. Also, the marine environment provides many uncertainties affecting the durability of the bridge. For instance, the salty water and air accelerate the corrosion of the structure. More research should be conducted in the next step.

Author details

Faham Tahmasebinia[1,2*], Yutaka Tsumura[1], Baichuan Wang[1], Yang Wen[1], Cheng Bao[1], Samad Sepasgozar[2] and Fernando Alonso-Marroquin[1]

1 School of Civil Engineering, The University of Sydney, Sydney, NSW, Australia

2 Faculty of Built Environment, The University of New South Wales, Sydney, NSW, Australia

*Address all correspondence to: faham.tahmasebinia@sydney.edu.au

References

[1] Watanabe E et al. Yumemai floating swing arch bridge of Osaka, Japan. In: Large Floating Structures. Singapore: Springer; 2015. pp. 61-90

[2] You D et al. Global, regional, and national levels and trends in under-5 mortality between 1990 and 2015, with scenario-based projections to 2030: A systematic analysis by the UN Inter-agency Group for Child Mortality Estimation. The Lancet. 2015; **386**(10010):2275-2286

[3] Bhadeshia H. Bulk nanocrystalline steel. Ironmaking & Steelmaking. 2005; **32**(5):405-410

[4] Tsuji N. Unique mechanical properties of nanostructured metals. Journal of Nanoscience and Nanotechnology. 2007;**7**(11):3765-3770

[5] Pham QP, Sharma U, Mikos AG. Electrospinning of polymeric nanofibers for tissue engineering applications: A review. Tissue Engineering. 2006;**12**(5): 1197-1211

[6] Standard Australia, AS5100.2-2004. Bridge design—Part 2: design loads. Sydney, Australia: Standards Australia; 2004

[7] Standards Australia. SAA Loading Code Part 2: Wind Loading. Australia: Standards Australia; 1989

[8] Zhang Q et al. A study of the effective elastic modulus of a lattice truss panel structure by experimental and theoretical analysis. Composite Structures. 2017;**165**:130-137